nature communications

Article

https://doi.org/10.1038/s41467-024-51807-7

# Sintilimab in combination with stereotactic body radiotherapy and granulocyte-macrophage colony-stimulating factor in metastatic non-small cell lung cancer: The multicenter SWORD phase 2 trial

Received: 3 March 2024

Accepted: 19 August 2024

Published online: 22 August 2024

Check for updates

Jianjiao Ni[1,2], Xiaofei Wang[3], Lin Wu[4], Xinghao Ai[5], Qian Chu[6], Chengbo Han[7], Xiaorong Dong[8], Yue Zhou[1,2], Yechun Pang[1,2] & Zhengfei Zhu[1,2,9]

This single-arm, multicenter, phase 2 trial (NCT04106180) investigated the triple combination of sintilimab (anti-PD1 antibody), stereotactic body radiotherapy (SBRT) and granulocyte-macrophage colony-stimulating factor (GM-CSF) in metastatic non-small cell lung cancer (NSCLC). With a median follow-up of 32.1 months, 18 (36.7%, 90% CI 25.3%–49.5%) of the 49 evaluable patients had an objective response, meeting the primary endpoint. Secondary endpoints included out-of-field (abscopal) response rate (ASR), progression-free survival (PFS), overall survival (OS), and treatment-related adverse events (TRAEs). The ASR was 30.6% (95% CI 18.3%–45.4%). The median PFS and OS were 5.9 (95% CI 2.5–9.3) and 18.4 (95% CI 9.7–27.1) months, respectively. Any grade and grade 3 TRAEs occurred in 44 (86.3%) and 6 (11.8%) patients, without grade 4–5 TRAEs. Moreover, in pre-specified biomarker analyses, SBRT-induced increase of follicular helper T cells (Tfh) in unirradiated tumor lesions and patient's blood, as well as of circulating IL-21 levels, was found associated with improved prognosis. Taken together, the triple combination therapy was well tolerated with promising efficacy and Tfh may play a critical role in SBRT-triggered anti-tumor immunity in metastatic NSCLC.

Immunotherapy targeting programmed cell death protein 1 (PD-1) or its ligand (PD-L1), has changed the treatment paradigm of non-small cell lung cancer (NSCLC)[1]. PD-1/PD-L1 inhibitors, including Sintilimab and others, have demonstrated treatment efficacy against advanced NSCLC[2,3]. However, primary and acquired resistance to PD-1/PD-L1 inhibitors frequently occurs, highlighting an urgent need to develop novel therapeutic combinations for advanced NSCLC[4].

[1]Department of Radiation Oncology, Fudan University Shanghai Cancer Center, Shanghai, China. [2]Department of Oncology, Shanghai Medical College, Fudan University, Shanghai, China. [3]Department of Biostatistics & Bioinformatics, Duke University School of Medicine, Durham, NC, USA. [4]The Second Department of Thoracic Oncology, Hunan Cancer Hospital, The Affiliated Cancer Hospital of Xiangya School of Medicine, Central South University, Changsha, China. [5]Shanghai Lung Cancer Center, Shanghai Chest Hospital, Shanghai Jiao Tong University, Shanghai, China. [6]Department of Oncology, Tongji Hospital, Tongji Medical College, Huazhong University of Science and Technology, Wuhan, China. [7]Department of Oncology, Shengjing Hospital of China Medical University, Shenyang, China. [8]Cancer Center, Union Hospital, Tongji Medical College, Huazhong University of Science and Technology, Wuhan, China. [9]Institute of Thoracic Oncology, Fudan University, Shanghai, China. e-mail: fuscczzf@163.com

Potential synergistic effects of PD-1/PD-L1 inhibitors and radiotherapy have been shown in NSCLC. Particularly, stereotactic body radiotherapy (SBRT), with the advantages of higher radiation dose per fraction and shorter duration, could release more tumor-associated antigens, cytokines, and T cell-attracting chemokines to enhance antitumor immunity[5]. Several prospective clinical trials have demonstrated promising results of combination therapy consisting of SBRT and PD-1/PD-L1 inhibitors, with an increase in overall response rate (ORR) and prolonged survival in advanced NSCLC[6,7]. Nevertheless, the treatment efficacy from these studies is still unsatisfactory, demanding novel therapeutic agents targeting non-redundant immune modulatory pathways.

Granulocyte-macrophage colony-stimulating factor (GM-CSF) promotes the differentiation, maturation, and expansion of dendritic cells (DCs) and triggers DCs to recognize process, and present tumor antigens to T cells, which further enhances the anti-tumor immunity triggered by radiotherapy[8]. In a proof-of-principle trial, a combination of GM-CSF and radiotherapy resulted in abscopal response in 4 of the 11 NSCLC patients, including 2 complete abscopal responses[9]. Additionally, preclinical and clinical studies showed enhanced anti-tumor response by the treatment of PD-1 inhibitors and GM-CSF via promoting T cell infiltration[10,11].

The SWORD trial was launched to investigate the efficacy and safety of the triple combination therapy in metastatic NSCLC. The safety run-in phase found that it was well tolerated with manageable treatment-related adverse events (TRAEs)[12]. Here we report the efficacy and final safety profile of the triple combination therapy, as well as results from translational investigations.

## Results

### Patient characteristics

Fifty-five patients were enrolled in this trial from six academic centers and of them 51 patients received at least one cycle of the assigned treatment (Fig. 1, supplementary Table 1). The trial was closed early due to slow accrual. The baseline demographics and clinical characteristics of patients in the full safety population were summarized in Supplementary Table 2. Of note, 37 (72.5%) patients had more than 3 metastatic organs and 42 (90.2%) had more than 5 metastatic lesions at baseline. The tumor sites irradiated by SBRT during the current study included the lung ($n = 20$, 39.2%), regional lymph node ($n = 16$, 31.4%), pleural nodule ($n = 5$, 9.8%), vertebra ($n = 3$, 5.9%), distant lymph node ($n = 3$, 5.9%), liver ($n = 2$, 3.9%), and others ($n = 2$, 3.9%) (Supplementary Table 3).

By the time of data cut-off, treatment had been discontinued in 49 patients and the rest 2 patients were still on Sintilimab treatment (Fig. 1). The median duration of GM-CSF and Sintilimab treatment was 14 (IQR 7–14) days and 5.7 (IQR 2.7–10.2) months, respectively.

### Treatment efficacy

With a median follow-up of 32.1 (IQR 6.6–36.4) months, 49 (96.1%) of the 51 patients were evaluable, and confirmed partial response (PR) was observed in 18 patients, without complete response (CR), contributing to an ORR of 36.7% (90% CI 25.3%–49.5%, 95% CI 23.4%–51.7%). Since the lower boundary of the ORR exceeded 20%, the current trial met the primary endpoint (Fig. 2A). Stable disease (SD) was documented in 15 patients with a disease control rate (DCR) of 67.3% (95% CI 52.5%–80.1%). Meanwhile, abscopal CR and PR occurred in 5 (10.2%) and 10 (20.4%) patients, respectively (Fig. 2B), leading to an out-of-field (abscopal) response rate (ASR) of 30.6% (95% CI 18.3%–45.4%).

By the date of data cut-off, 40 patients had disease progression and the median progression-free survival (PFS) was 5.9 (95% CI 2.5–9.3) months. Of note, 5 of the 49 patients completed 2 years of Sintilimab treatment, 2 of whom were still free of progressive disease (Fig. 2C). The 6-month, 12-month, and 18-month PFS rates were 48.8% (95% CI 41.4%–56.2%), 31.7% (95% CI 24.6%–38.8%), and 23.8% (95% CI 17.2%–30.4%), respectively (Fig. 2D).

Additionally, 29 patients had died and the median overall survival (OS) was 18.4 (95% CI 9.7–27.1) months. The 12-month, 24-month, and 36-month OS rates were 75.5% (95% CI 69.4%–81.6%), 56.1% (95% CI 48.9%–63.3%), and 43.7% (95% CI 36.2%–51.2%), respectively (Fig. 2E). Meanwhile, 46 (93.9%) of the 49 evaluable patients had baseline PD-L1 expression data and treatment efficacy in these 46 patients stratified by baseline PD-L1 expression levels were summarized in Supplementary Table 4.

### Safety

Among the 51 patients in the full safety population, 44 (86.3%) experienced any grade TRAEs (Supplementary Table 5), the most frequent of which included fatigue (37.3%), fever (29.4%), ostealgia (17.6%), and rash (11.8%). Grade 3 TRAEs occurred in 6 (11.8%) patients, including ALT elevation (3.9%), AST elevation (3.9%), leucopenia (3.9%), neutropenia (3.9%), creatinine increase (2.0%), pneumonitis (2.0%), and acute heart failure (2.0%). No grade 4–5 TRAE occurred. Severe adverse events (grade 3 pneumonitis and hepatitis) developed in 1 (2.0%) patient without previous history of relevant pulmonary or hepatic disease after the third cycle of Sintilimab treatment, resulting in admission to the hospital. The patient gradually recovered after treatment with corticosteroids and Sintilimab was permanently discontinued.

Any grade and grade 3 immune-related AEs occurred in 32 (62.8%) and 3 (5.9%) patients, respectively. TRAEs led to the discontinuation of Sintilimab treatment in 5 patients (pneumonitis = 4, myocarditis = 1) and GM-CSF in 3 patients (acute heart failure = 2, white blood cell increase = 1). Notably, GM-CSF-induced acute heart failure occurred in 2 patients enrolled for the safety run-in phase, which was transient and resolved within 7 days after diuretic treatment[12].

### Biomarker analyses

Biomarker analyses using serially collected tissue and blood samples were pre-specified exploratory endpoints. In fact, paired blood samples were available from 37 patients, and paired tissue samples were successfully obtained in 21 of the 37 patients. RNA sequencing was performed using the 42 tissue samples and 244 differentially expressed genes (DEGs) were identified (Supplementary Fig. 1A). Kyoto Encyclopedia of Genes and Genomes (KEGG) (Supplementary Fig. 1B) and Gene Ontology (GO) (Supplementary Fig. 1C) enrichment analyses revealed significant enrichment of DEGs in several signaling pathways, including those related to immune regulation.

Subsequently, the relative abundance of 22 infiltrating immune cells in the pre-SBRT and post-SBRT tissue samples were enumerated using CIBERSORT (Fig. 3). A significant SBRT-induced increase of follicular helper T cells (Tfh) and activated natural killer (NK) cells was found. The median frequencies of Tfh and activated NK cells in the unirradiated tumor lesions increased from 2.54% (IQR 0.35%–3.57%) to 3.86% (IQR 2.84%–5.51%) ($p = 0.026$), and from 2.06% (IQR 0.11%–4.33%) to 3.52% (IQR 0.15%–6.98%) ($p = 0.014$), respectively. Moreover, a higher frequency of Tfh, as well as activated NK cells in the post-SBRT tissue samples (Fig. 4B), but not in the pre-SBRT tissue samples (Fig. 4A), was associated with improved OS. Additionally, a higher frequency of Tfh in the post-SBRT tissue samples was associated with a longer PFS (Fig. 4B). No other significant association was found between the relative abundance of infiltrating immune cells in the tissue samples and survival outcomes.

To investigate the functional state of different stromal cells, the relative abundance of 71 transcriptionally-defined cell states in the pre-SBRT and post-SBRT tissue samples were enumerated using EcoTyper (Fig. 5). Several significantly deregulated cell states, including CD4 T cell (S03), endothelial cell (S05), fibroblast cell (S02), mast cell (S01),

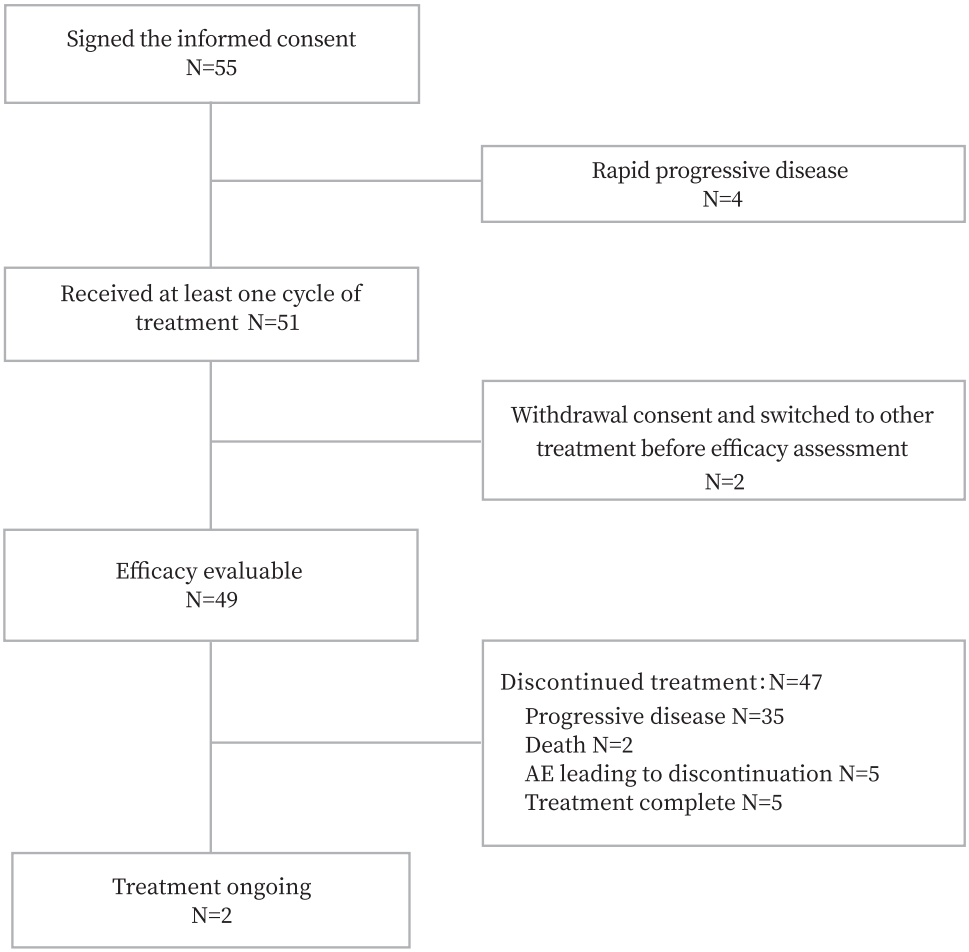


**Fig. 1** | Patient enrollment flowchart. AE adverse events.

monocytes/macrophages (S05), and plasma cell (S01), were found. Specifically, the median frequency of CD4 T cell (S03) in the unirradiated tumor lesions increased from 0.37% (IQR 0.00%–2.26%) to 0.46% (IQR 0.00%–13.46%) ($p = 0.049$). Of note, one of the top 5 genes coding the specific cell surface proteins for this cell state is *ITGA1* (encoding CD49a), which was repeatedly found to be involved in the regulation of T cell function[13,14]. Moreover, a higher frequency of CD4 T cell (S03), as well as B cell (S03), in the post-SBRT tissue samples (Fig. 6B), but not in the pre-SBRT samples (Fig. 6A), was significantly associated with improved PFS and OS. No other significant association was found between the relative abundance of cell states in the tissue samples and survival outcomes.

Enzyme-linked immunosorbent assay (ELISA) was performed using the 74 blood samples, and the levels of interleukin (IL)-2, IL-5, IL-10, IL-12, IL-17, interferon (IFN)-α, and IFN-β were under the lower limit in most of the samples, thus excluded from further analyses. The concentrations of circulating IL-2 receptor (IL-2R) and IL-21 were significantly elevated after SBRT (Fig. 7A). Moreover, a higher level of circulating IL-2R, as well as IL-21, in the post-SBRT plasma samples (Fig. 7C), but not in the pre-SBRT plasma samples (Fig. 7B), was significantly associated with improved PFS and OS. Meanwhile, a higher level of circulating IL-8, as well as a lower level of exosomal PD-L1, in the pre-SBRT and post-SBRT blood samples, was associated with the improved PFS and OS, although the association between circulating IL-8 in the pre-SBRT blood samples and OS did not reach statistical significance (Supplementary Fig. 2). No other significant association was found between the concentration of circulating cytokines and survival outcomes.

Taken together, Tfh/IL-21 signaling may be involved in the modulation of SBRT-triggered immune response. Since all of the tissue samples were sent for RNA sequencing, we tried to preliminarily test this hypothesis using the blood samples. The frequency of circulating Tfh, a generally acceptable counterpart for the investigation of Tfh disorders in various disease models[15,16], and the expression of CD49a, were measured using flow cytometry (Supplementary Fig. 3). SBRT-induced increase of circulating Tfh and CD49a expression were found (Fig. 8A) and a positive correction between the abundance of infiltrating Tfh in the post-SBRT tissue samples and the frequency of circulating Tfh in the post-SBRT blood samples was discovered ($p = 0.013$, Fig. 8B). Similarly, patients with a higher level of circulating Tfh also tended to have an elevated level of circulating IL-21 in the post-SBRT blood samples ($p = 0.062$, Fig. 8B). Furthermore, an increased expression of CD49a in the post-SBRT blood samples was associated with a numerically longer survival (Fig. 8C). No other significant association was found between the circulating parameters and survival outcomes.

Besides, GSE161537 contained targeted RNA sequencing data from 82 metastatic NSCLC patients treated with second-line PD-1/PD-L1 inhibitors[17,18]. The median frequency of infiltrating Tfh, estimated using CIBERSORT, was 3.21% (IQR 0.61%–5.49%) and a higher frequency of Tfh was associated with prolonged OS in GSE161537 ($p = 0.015$, Supplementary Fig. 4).

## Discussion

In the current study, we found that the triple combination therapy consisting of a PD-1 inhibitor, SBRT, and GM-CSF in advanced NSCLC

https://doi.org/10.1038/s41467-024-51807-7

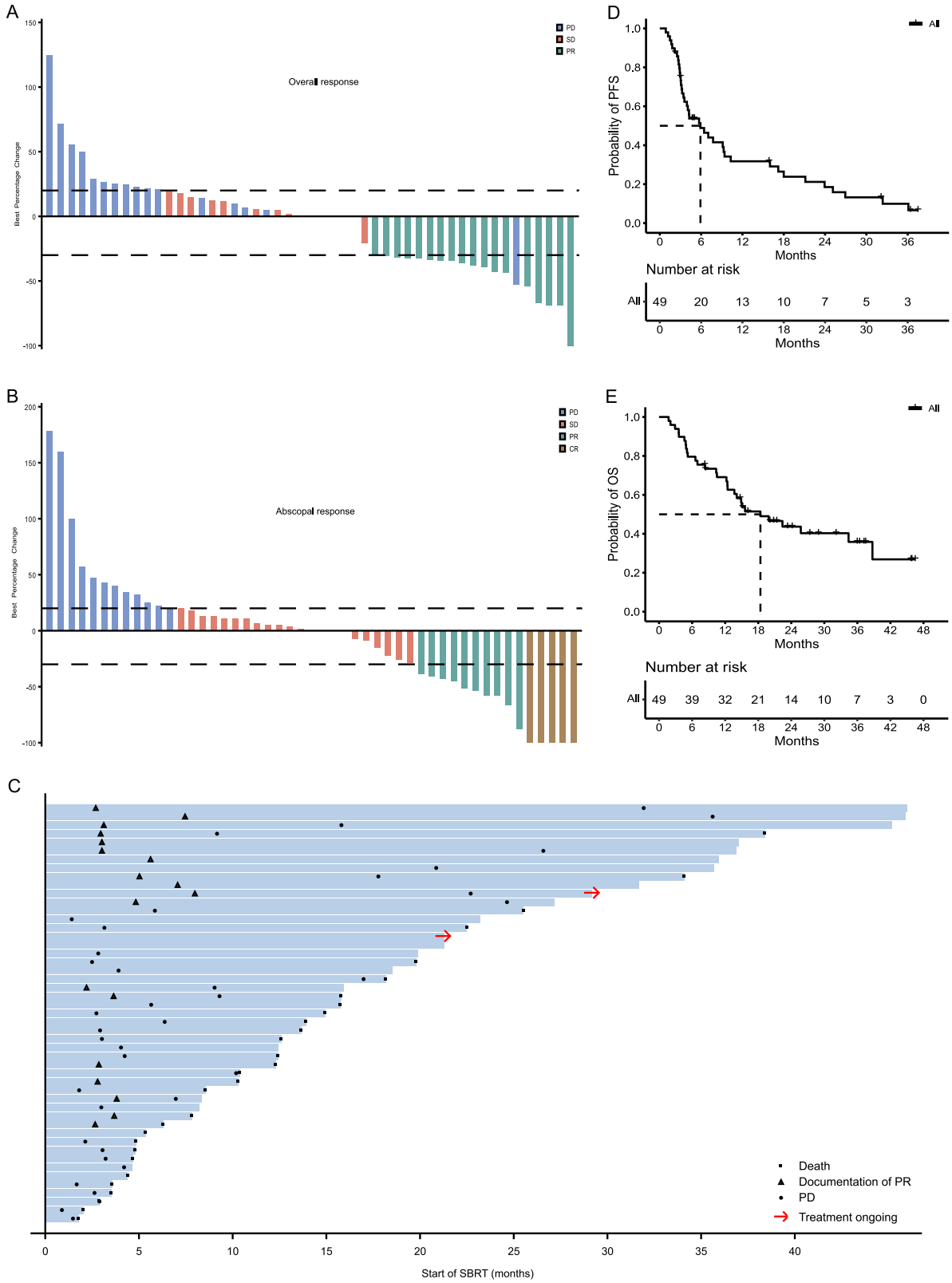


**Fig. 2 | Response and survival outcomes in evaluable patients ($n = 49$). A** Best overall response. **B** Best abscopal response. **C** Swimmer plots. **D** Progression-free survival (PFS). **E** Overall survival (OS). Source data are provided in the Source Data file.

was associated with improved ORR and manageable safety profiles when compared with historical control of PD-1 inhibitor monotherapy[19–21]. Furthermore, Tfh was found to be potentially involved in the regulation of SBRT-triggered systemic anti-tumor immune response, which warranted future validation.

First of all, this trial met the pre-specified primary endpoint with clinically meaningful improvement in treatment efficacy. Historically, the ORRs of anti-PD-1 monotherapy in unselected metastatic NSCLC ranged from 17% to 20%[19–22]. For example, the ORR was 20% in the ORIENT-3 study, which investigated Sintilimab monotherapy among

https://doi.org/10.1038/s41467-024-51807-7

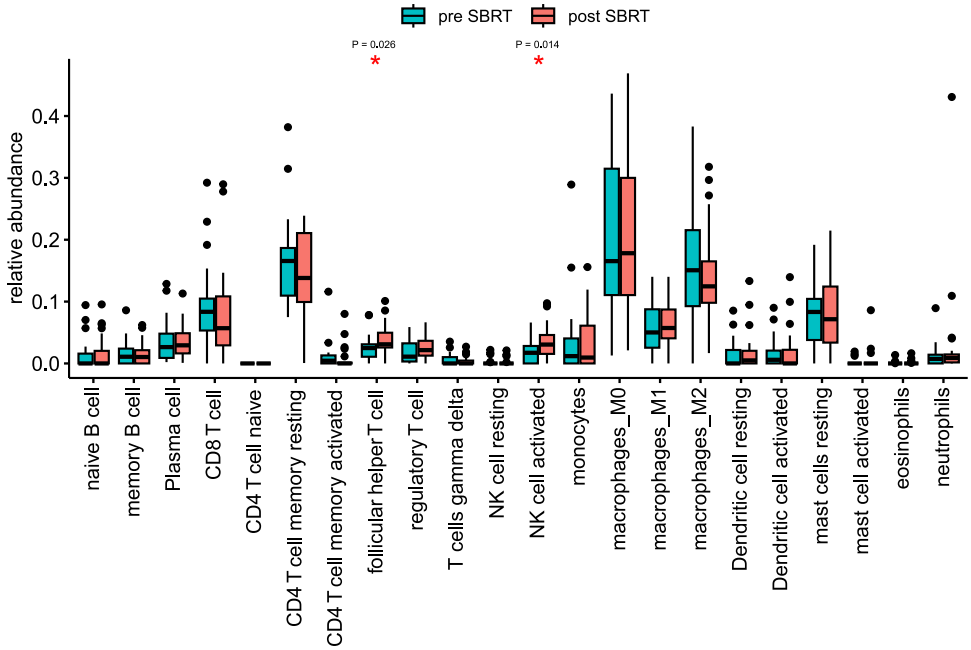


**Fig. 3 | The landscape and dynamic changes of infiltrating immune cells estimated using CIBERSORT in the unirradiated tumor lesions before and after stereotactic body radiotherapy (SBRT).** Forty-two paired tissue samples were collected from 21 patients. *P*-value < 0.05 (two-sided) was considered statistically significant using the Wilcoxon test. The exact *P*-values for immune cells with significant SBRT-related changes were displayed. The median, first quartile (Q1), third quartile (Q3), whiskers (minima = Q1 − 1.5IQR, maxima = Q3 + 1.5IQR), and outliers (1.5 times the IQR less than the first quartile, or 1.5 times the IQR greater than the third quartile) were presented. Raw data of RNA sequencing are now available at the GSA-Human dataset HRA006932. IQR interquartile range.

locally advanced or metastatic squamous-cell NSCLC after failure of first-line chemotherapy[22]. The ORR was 36.7% in the current study, which was superior to these historical controls and generally comparable to the reported ORRs from prospective trials investigating combination therapy of SBRT and PD-1/PD-L1 inhibitors in advanced NSCLC, such as the PEMBRO-RT study (36.0%)[6,23]. Similarly, the survival outcomes of the current study seemed to be longer than those of historical controls of anti-PD-1 monotherapy and were consistent with those of combined SBRT and PD-1/PD-L1 inhibitors[6,19–23]. All of these data supported the potential synergistic effect between SBRT and PD-1/PD-L1 inhibitors in advanced NSCLC. Based on these promising results, a randomized controlled trial (The RADIUM study, NCT06313541) has been initiated by our group to investigate the efficacy and safety of chemoimmunotherapy plus individualized radiotherapy in untreated driver-mutation-negative metastatic NSCLC.

Nevertheless, the exact clinical value of GM-CSF treatment in the triple combination therapy could not be asserted. Accumulating evidence suggests that GM-CSF could promote the maturation and activation of various kinds of anti-tumor immune cells, such as DCs, T cells, and NK cells[8,24,25]. Hence, the triple combination therapy was initially designed to target non-redundant immune modulatory pathways, including promoting the release of tumor-associated antigens, activating distinct innate immune responses, and rejuvenating the suppressed tumor immune microenvironment. However, the treatment efficacies of the current triple combination therapy, in terms of ORR, PFS, and OS, seemed to be similar to those of combined PD-1/PD-L1 inhibitors with SBRT, indicating a lack of extra clinical benefit of GM-CSF. However, 90.2% and 72.5% of the patients enrolled in the current study had more than 5 metastatic lesions and more than 3 metastatic organs at baseline, representing a high tumor burden, which was found to be associated with worse prognosis among immunotherapy-treated metastatic NSCLC[26–28]. Therefore, GM-CSF treatment may have certain clinical value in the triple combination therapy, since the current regimen achieved similar treatment outcomes in a cohort of patients presumed to be with compromised prognosis. Meanwhile, only one cycle of GM-CSF treatment was administered, concurrently with Sintilimab, in the current study. The clinical utility of GM-CSF with different dosages and treatment sequences needs to be further investigated.

Secondly, the triple combination therapy was well tolerated, without grade 4–5 TRAEs. Grade 3 TRAEs and grade 3 immune-related AEs occurred in 11.8% and 5.9% of the patients, which was comparable to those treated with anti-PD-1 monotherapy[19–22] or combined therapy of PD-1/PD-L1 inhibitors with SBRT[6,23]. Of note, ostealgia, a common TRAE of GM-CSF[29], occurred in 17.6% of the patients, all of which were mild and manageable. Similarly, acute heart failure that occurred in 2 (3.9%) patients, was probably due to GM-CSF that had been extensively discussed previously[12]. Since more than 70% of the patients received thoracic SBRT, special attention should be paid to the occurrence of pneumonitis. The incidences of any grade (9.8%) and grade 3 (2.0%) pneumonitis, were generally similar to those reported in patients treated with anti-PD-1 monotherapy[19–22]. A recent pooled analysis of trials from the US Food and Drug Administration Database, which included individual patient data of 16835 patients, assessed the association of radiotherapy with the risk of adverse events in patients who received immunotherapy. No significant difference in the incidence of TRAEs, especially grade 3–4 TRAEs, was found between patients who received radiotherapy and not[30]. With the improvement of SBRT techniques and toxicity monitoring strategies, TRAEs of the combination therapy are increasingly manageable.

Distinct signaling pathways and immune cells have been connected to the radiotherapy-induced abscopal effects[31,32]. Nevertheless, the associations between Tfh and radiotherapy-induced abscopal effects are largely unknown. Previously, irradiation was found to increase the abundance of Tfh, as well as the secretion of IL-21, in various human tissues and cell lines[33,34]. Here we report a significant SBRT-induced elevation of Tfh abundance in the unirradiated tumor lesions and patient's blood, along with a dramatic increase in circulating IL-21 levels. Meanwhile, accumulating evidence has demonstrated a critical role of Tfh in promoting anti-tumor immune response

https://doi.org/10.1038/s41467-024-51807-7

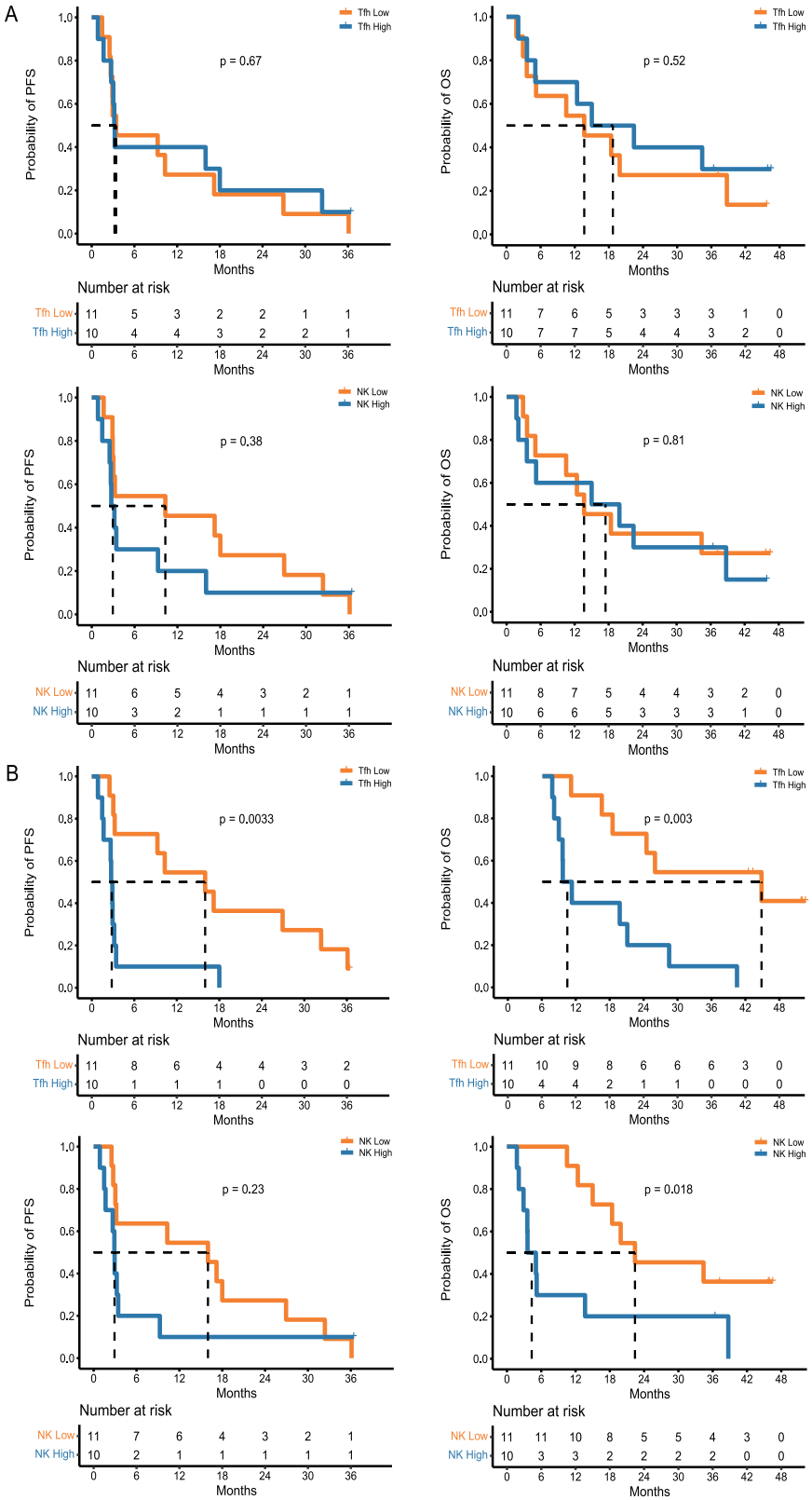


**Fig. 4 | The prognostic significance of infiltrating follicular helper T cells (Tfh) and activated natural killer cells (NK) in the unirradiated tumor lesions ($n = 21$).** The associations of relative abundance of infiltrating Tfh and activated NK with the patient's progression-free survival (PFS) and overall survival (OS), in the pre-SBRT (**A**) and post-SBRT (**B**) tissue samples (log-rank test). *P*-value < 0.05 (two-sided) was considered statistically significant without adjustment for multiplicity. Source data are provided in the Source Data file. SBRT stereotactic body radiotherapy.

https://doi.org/10.1038/s41467-024-51807-7

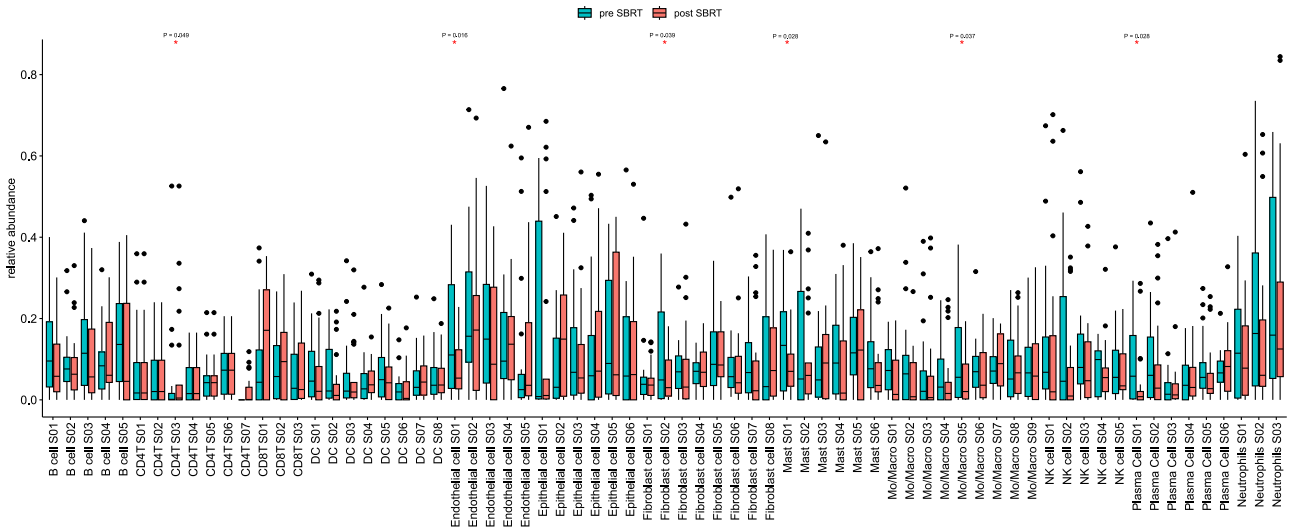


**Fig. 5 | The landscape and dynamic changes of cell states estimated using EcoTyper in the unirradiated tumor lesions before and after stereotactic body radiotherapy (SBRT).** Forty-two paired tissue samples were collected from 21 patients. *P*-value < 0.05 (two-sided) was considered statistically significant using the Wilcoxon test. The exact *P*-values for cell states with significant SBRT-related changes were displayed. The median, first quartile (Q1), third quartile (Q3), whiskers (minima = Q1 − 1.5IQR, maxima = Q3 + 1.5IQR), and outliers (1.5 times the IQR less than the first quartile, or 1.5 times the IQR greater than the third quartile) were presented. Raw data of RNA sequencing are now available at the GSA-Human dataset HRA006932. IQR interquartile range.

in various human cancers, including NSCLC[35–37]. Tumor neoantigens could regulate the fate of tumor-specific Tfh by facilitating their interactions with tumor-specific B cells, which in turn could promote anti-tumor immunity by enhancing CD8 T cell effector functions[35]. Moreover, Tfh was found to be essential for the efficacy of PD-1/PD-L1 inhibitors in NSCLC, since Tfh could accumulate in the tumor bed drain lymph nodes, and produce IL-21, which could sustain the proliferation, viability, cytokine production, and cytotoxic functions of exhausted T cells[36,38]. In the current study, the relative abundance of infiltrating Tfh in the post-SBRT tissue samples, as well as the circulating IL-21 levels in the post-SBRT blood samples, were significantly associated with survival outcomes, collaborating with previous studies.

Intriguingly, a specific cell state, CD4 T cell (S03), characterized by the expression of CD49a, was significantly increased in the post-SBRT samples and associated with improved prognosis, indicating a potential link between CD49a expression and Tfh activation in the modulation of SBRT-triggered immune response[13,39,40]. In fact, CD49a expression was found to be associated with the differentiation and activation of T cells in various disease models, including human cancers[13,14,41,42]. Based on the preliminary results from the current study, we hypothesized that CD49a may define a functional subset of Tfh that actively participates in the modulation of SBRT-triggered immune response, warranting further investigation. Meanwhile, the levels of circulating IL-8 and exosomal PD-L1 were found to be potential prognostic factors of metastatic NSCLC receiving immunotherapy in the current study, reconfirming previous findings[43–45].

The relative abundance of infiltrating immune cells and cell states were estimated using bioinformatic tools (i.e., CIBERSORT and EcoTyper), but not validated through direct methods such as flow cytometry or immunohistochemistry, due to the lack of adequate tissue samples. In addition, the quantity and functional state of circulating Tfh were measured by a limited panel of surface makers. However, the results generated from RNA sequencing data, circulating cytokine profiling, and flow cytometrical analyses were generally consistent. The relative abundance and prognostic significance of infiltrating Tfh were preliminarily validated by an external dataset. All of these data provided important hints for the elucidation and optimization of the synergistic effect between PD-1/PD-L1 inhibitors and SBRT in metastatic NSCLC.

There were several limitations in this study. Firstly, no control arm was included, which limited the interpretation of the specific contribution of each study drug. Especially, the clinical value of GM-CSF in combination therapy has to be further investigated. Secondly, since this was a hypothesis-generating phase II study with a relatively small sample size, no specific statistical model was used to handle the missing data, and the *p*-values were not adjusted for multiplicity in the biomarker analyses. Additionally, only a fixed SBRT dose-fractionation targeting a single tumor site was allowed in the current study. Distinct radiotherapy schedules may have different immune-modulating effects, and conflicting results were reported in NSCLC[7,46,47]. Large randomized clinical trials exploring the optimal schedule of combining radiotherapy and immunotherapy in NSCLC are ongoing (NCT03774732, NCT05111197, NCT04929041, and others).

In conclusion, the SWORD trial met its primary endpoint, indicating potentially improved treatment efficacy with the triple combination therapy of Sintilimab, SBRT, and GM-CSF in previously treated, EGFR/ALK mutation-negative, metastatic NSCLC patients. Tfh may play a critical role in the modulation of SBRT-triggered anti-tumor immune response, which warranted future investigation.

## Methods

### Study design

The study was conducted in accordance with the Department of Health and Human Services, the Declaration of Helsinki, and all relevant ethical regulations. Informed consent was obtained from each patient prior to the commencement of study activities. The institutional review boards of Fudan University Shanghai Cancer Center, Hunan Cancer Hospital, Tongji Hospital of Tongji Medical College, Shengjing Hospital of China Medical University, Shanghai Chest Hospital, Union Hospital of Tongji Medical College approved the study.

The design of the SWORD trial (NCT04106180) was previously published[12]. Briefly, patients with EGFR/ALK mutation-negative metastatic NSCLC failing first-line platinum-based chemotherapy, having a tumor lesion suitable for SBRT at a dose of 24 Gy in 3 fractions and at least another measurable tumor lesion as per the Response Evaluation Criteria in Solid Tumors (RECIST) v1.1, were enrolled. Patients underwent SBRT once daily for three consecutive days, targeting a single extracranial tumor lesion, and Sintilimab (200 mg, Innovent Biologics

https://doi.org/10.1038/s41467-024-51807-7

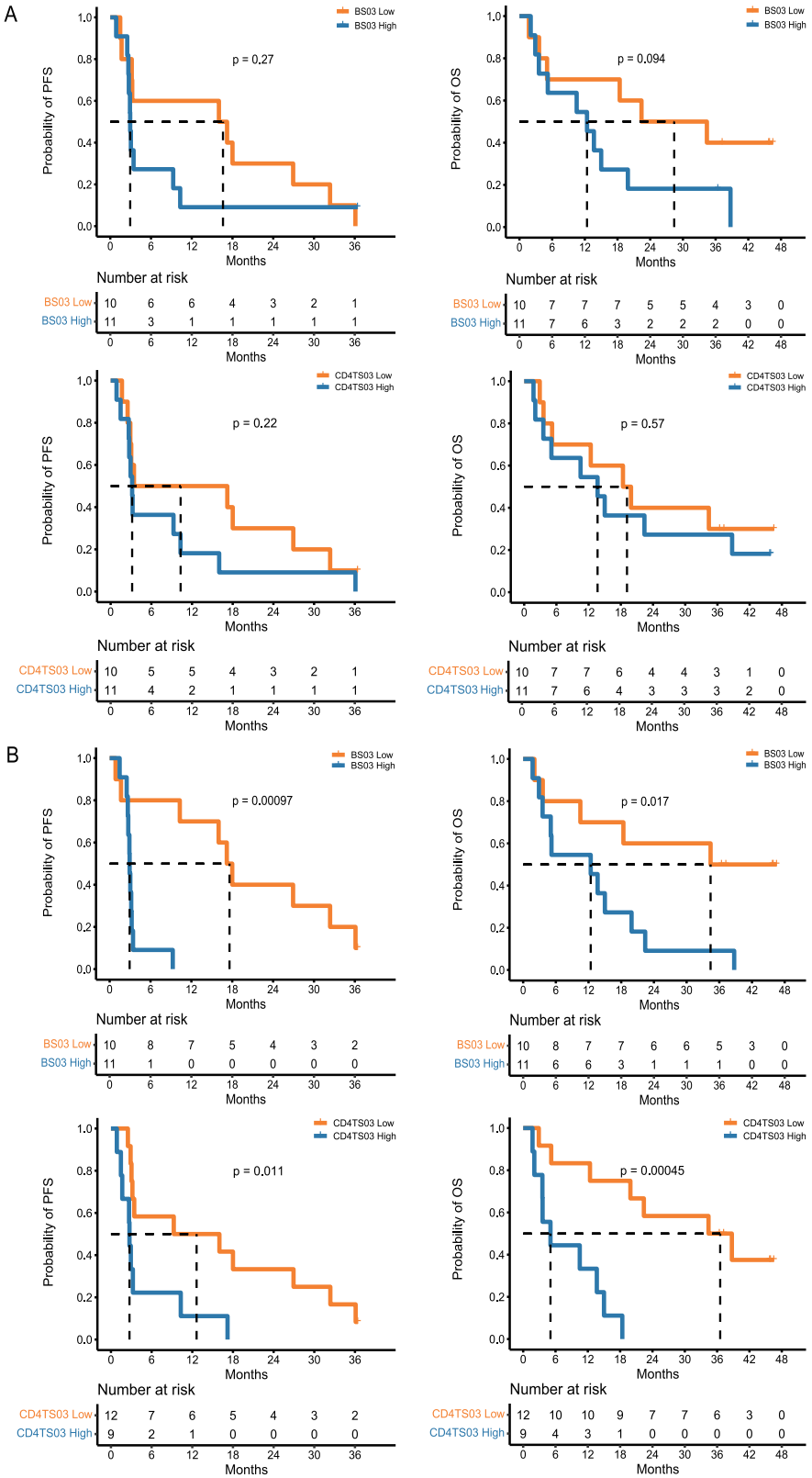


**Fig. 6 | The prognostic significance of B cells (S03) (BS03) and CD4 T cells (S03) (CD4TS03) in the unirradiated tumor lesions ($n = 21$).** The associations of relative abundance of BS03 and CD4TS03 with the patient's progression-free survival (PFS) and overall survival (OS), in the pre-SBRT (**A**) and post-SBRT (**B**) tissue samples (log-rank test). *P*-value < 0.05 (two-sided) was considered statistically significant without adjustment for multiplicity. Source data are provided in the Source Data file. SBRT, stereotactic body radiotherapy.

https://doi.org/10.1038/s41467-024-51807-7

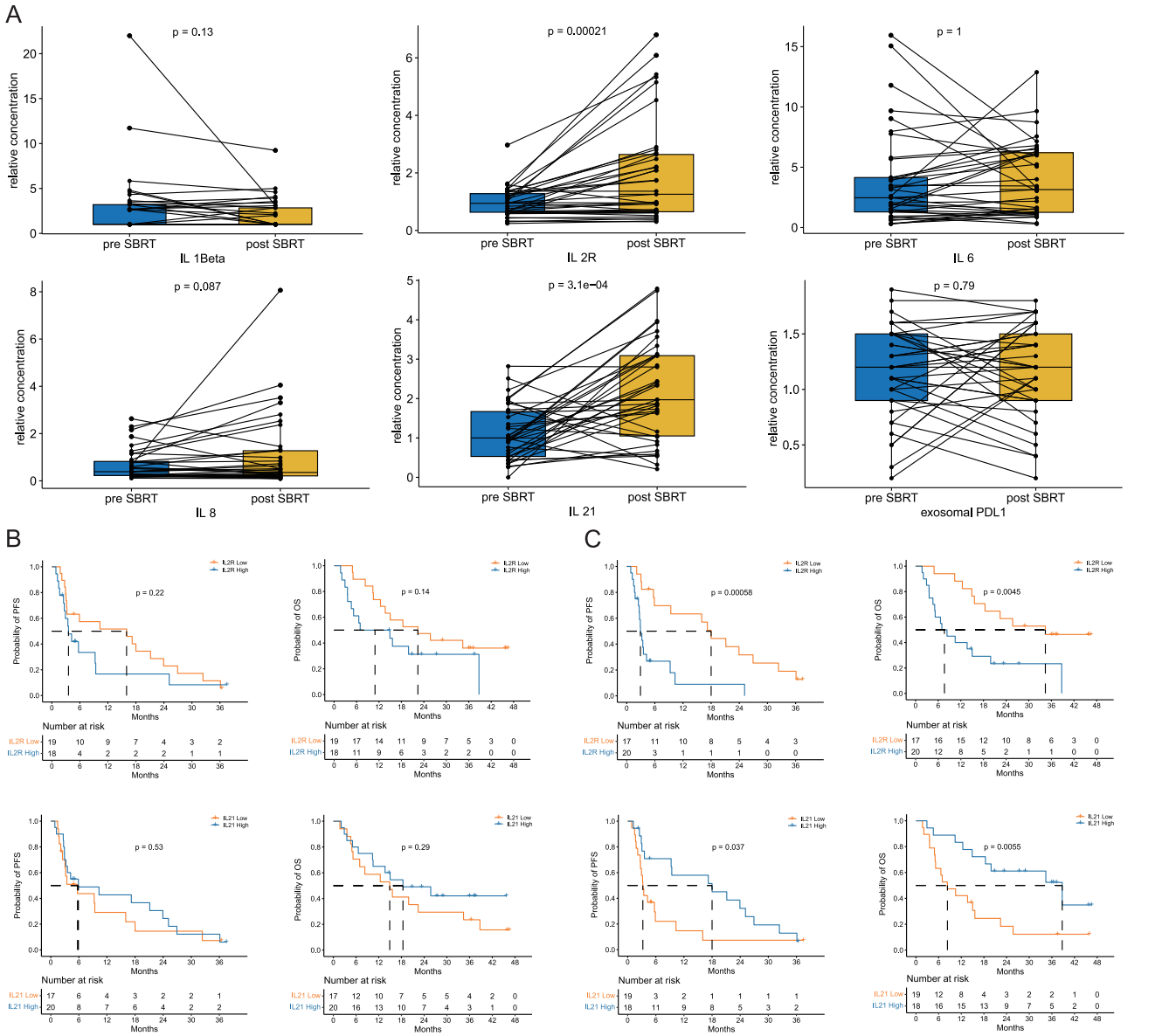


**Fig. 7 | Dynamic changes and their prognostic significances of circulating parameters.** Seventy-four paired blood samples were collected from 37 patients. **A** SBRT-induced changes of circulating cytokine levels and exosomal PD-L1 level (paired *t*-test). The median, first quartile (Q1), third quartile (Q3), whiskers (minima = Q1 − 1.5IQR, maxima = Q3 + 1.5IQR) were presented in the box plots. **B**, **C** The associations of circulating IL−2R and IL-21 levels with patient's progression-free survival (PFS) and overall survival (OS), in the pre-SBRT (**B**) and post-SBRT (**C**) blood samples (log-rank test). *P*-value < 0.05 (two-sided) was considered statistically significant without adjustment for multiplicity. Source data are provided in the Source Data file. SBRT, stereotactic body radiotherapy.

(Suzhou) Co., Ltd., China) was administered intravenously once every 3 weeks until disease progression, emergence of intolerable toxicity, consent withdrawal, death, or for up to 24 months, within 3 weeks after completion of SBRT. Recombinant human granulocyte/macrophage colony-stimulating factor (125 μg/m$^2$, Xiamen Amoytop Biotech Co., Ltd., China) was administered once daily until disease progression, emergence of intolerable toxicity, consent withdrawal, death, or for up to 14 consecutive days, starting at the same day of the first cycle of Sintilimab treatment. Complete follow-up, including physical examination, laboratory assessment, information on adverse events, and radiographic evaluation, was performed every 9 weeks. The participants were enrolled between October 16, 2019 and August 22, 2022. The data was cut off on August 31, 2023.

The primary endpoint was ORR, defined as the proportion of patients whose best overall response included either a confirmed CR or PR in all evaluable patients per RECISIT 1.1, similar to previous studies[19,20]. Secondary endpoints included TRAEs, PFS, OS, and ASR. ASR was defined as the proportion of patients with at least a 30% reduction in the longest diameter of any non-irradiated target lesions from the baseline value by the RECIST 1.1 at any efficacy assessment.

AEs were graded using the National Cancer Institute Common Terminology Criteria for Adverse Events (CTCAE) version 5.0 and documented in all patients receiving at least one dose of the assigned treatment (full safety population). Besides, a safety run-in phase was included to ensure that not many severe AEs happened in treated patients, and the results from which were previously published[12].

## Biomarker analyses

Biomarker evaluation was conducted as a pre-defined exploratory endpoint. Paired tissue samples from an unirradiated tumor lesion, as well as paired blood samples, were collected within 1 week before and

https://doi.org/10.1038/s41467-024-51807-7

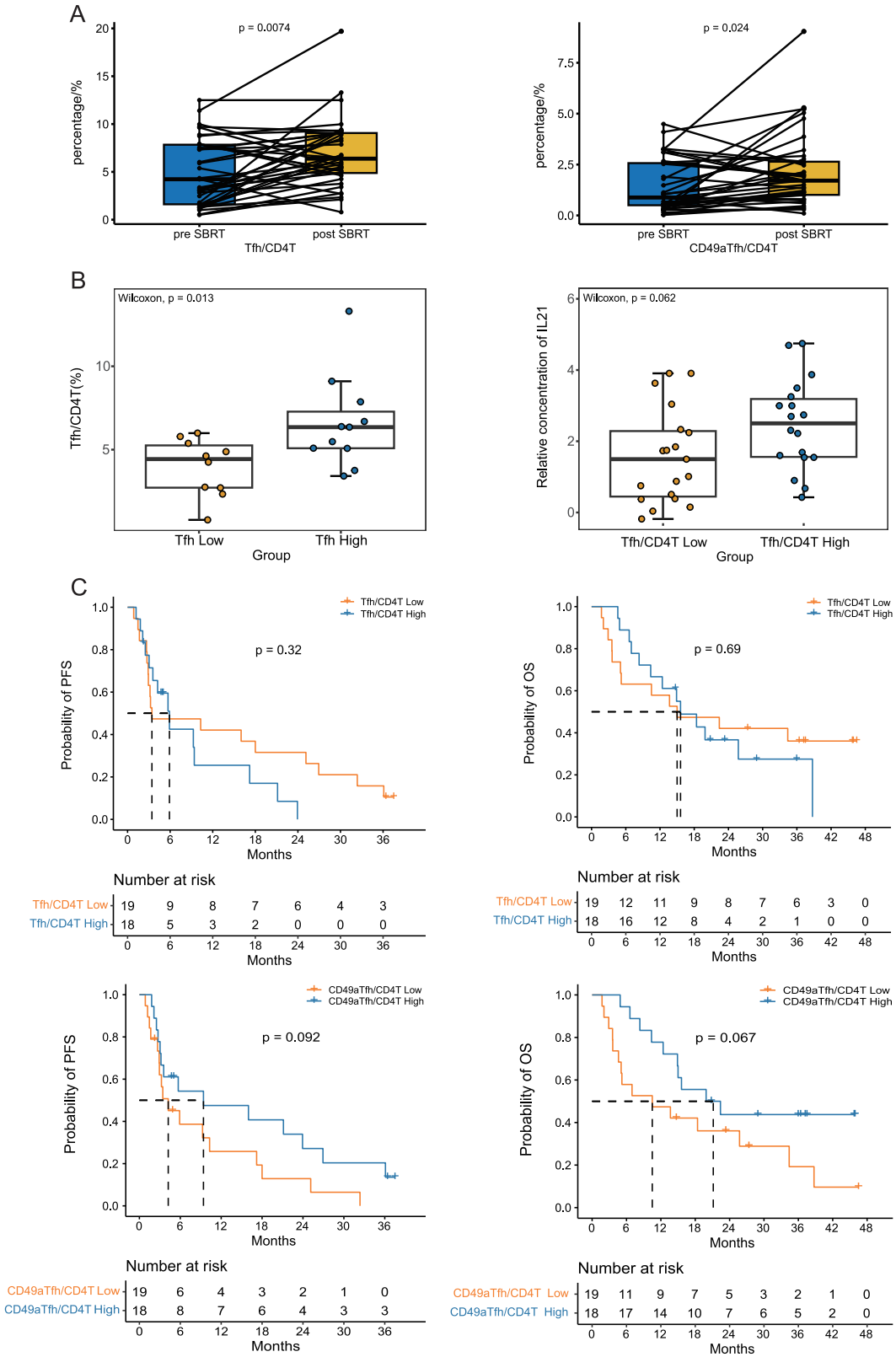


after SBRT (but before the initiation of the first cycle of Sintilimab and GM-CSF treatment). The dynamic changes and prognostic significances of parameters generated using these samples were extensively analyzed. Of note, the median values were selected as the cut-off when stratifying patients based on the expression levels and *P*-value < 0.05 was considered to be statistically significant in biomarker analyses.

### RNA sequencing, GO, and KEGG analyses

The tissue samples were promptly immersed in RNA-fix reagent and kept at −80 °C until utilization. After all samples were gathered, total RNA was isolated using TRIzol reagent (Invitrogen, Carlsbad, CA, USA). The quality of RNA was evaluated using RNA High-Sensitivity Screen on TapeStation (Agilent Technologies) and the libraries were constructed using Illumina TruSeq RNA Exome Library Prep Kit following the

**Fig. 8 | The dynamic changes and clinical significance of circulating follicular helper T cells (Tfh) and CD49a$^+$ Tfh.** Seventy-four paired blood samples were collected from 37 patients and 42 paired tissue samples were collected from 21 of the 37 patients, before and after stereotactic body radiotherapy (SBRT). **A** SBRT-induced changes of the percentages of circulating Tfh and CD49a$^+$ Tfh among circulating CD4$^+$ T cells (Wilcoxon test). **B** The correlations between the percentage of Tfh in the circulating CD4$^+$ T cells in the post-SBRT blood samples, with the relative abundance of infiltrating Tfh cells in the post-SBRT tissue samples (left), as well as with the circulating IL-21 levels in the post-SBRT blood samples (right) (Wilcoxon test). The median, first quartile (Q1), third quartile (Q3), and whiskers (minima = Q1 − 1.5IQR, maxima = Q3 + 1.5IQR) were presented in the box plots (**A**, **B**). **C** The associations of the percentages of Tfh and CD49a$^+$ Tfh in the circulating CD4$^+$ T cells with the patient's progression-free survival (PFS) and overall survival (OS) in the post-SBRT blood samples (log-rank test). *P*-value < 0.05 (two-sided) was considered statistically significant without adjustment for multiplicity. Source data are provided in the Source Data file.

manufacturer's protocols. Sequencing was then performed on an Illumina HiSeq 4000 platform and reads were aligned using HISAT2 (version 2.0.4). DEGs were identified using the DESeq2 R package (1.16.1). *P*-value < 0.05 and absolute fold-change of 2 were selected as the threshold for DEGs. The R package `pheatmap' was utilized to create a heatmap that illustrated the expression of DEGs.

Furthermore, KEGG analysis was a well-known database for systematic analysis of gene functions in biological pathways, which links genomic information with higher-order functional information. GO analysis was a common and useful method for annotating genes and gene products, and identifying characteristic biological attributes of high-throughput genome or transcriptome data. The DAVID online database (https://david.ncifcrf.gov/) was an essential online tool for high-throughput gene functional analysis, which provided the functionality to perform simultaneous KEGG and GO analysis[48]. In the current study, the DEGs were mapped to the relevant biological annotation using the DAVID online database. KEGG and GO enrichment analyses were performed using the cluster Profiler R package. *P*-value < 0.05 was considered statistically relevant.

### Estimation of infiltrating immune cells and cell states

CIBERSORT was an analytical tool to impute gene expression profiles and provide an estimation of the abundances of 22 immune cells in the tumor microenvironment, using gene expression data[49]. The relative abundance of infiltrating immune cells in the paired tissue samples from the same unirradiated tumor lesion were enumerated using CIBERSORT. Fragments Per Kilobase of transcript per Million mapped reads (FPKM)-normalized expression was used as the input data file. To run CIBERSORT, the following packages were required in R software: "e1071", "parallel", and "preprocessCore". A file called "LM22.txt", which contained a "signature matrix" of 547 genes, in R (obtained under Menu > Download from CIBERSORT, https://cibersort.stanford.edu/download.php) was also required[50].

EcoTyper was a machine learning framework for characterizing cell type-specific states and multicellular communities from bulk, single-cell, and spatially-resolved expression data[51]. The relative expression of the 71 transcriptionally-defined cell states in the paired tissue samples from the same unirradiated tumor lesion were enumerated using EcoTyper (https://ecotyper.stanford.edu/)[52]. FPKM-normalized expression was used as the input data file.

### ELISA

Cell-free plasma samples were obtained after centrifuging at 2000 × *g* for 10 min at 4 °C and stored at −80 °C until utilization. For patients with adequate plasma samples, concentrations of 13 circulating cytokines were measured using the ELISA. Human cytokine ELISA kits, including IL-1β, IL-2, IL-2R, IL-5, IL-6, IL-8, IL-10, IL-12, IL-17, IL-21, tumor necrosis factor (TNF)-α, IFN-α, and IFN-β, were purchased from Invitrogen (Carlsbad, CA, USA), and the concentrations of these cytokines were measured according to the manufacturer's instructions. Besides, exosomes were collected from plasma samples by differential centrifugation and the concentration of exosomal PD-L1 was measured using an Invitrogen human PD-L1 ELISA Kit[43].

### Flow cytometry

The frequency of immune cells that were revealed to be potentially involved in the regulation of SBRT-triggered abscopal effects based on the results from RNA sequencing and circulating cytokines profiling, was determined in the blood samples using flow cytometry. For patients with adequate blood samples, peripheral blood mononuclear cells (PBMCs) were isolated by Ficoll-Paque density gradient centrifugation. PBMCs were washed and resuspended in fetal calf serum containing 10% dimethyl sulfoxide (DMSO, SIGMA, Cat#276855) for storage at −80 °C until utilization.

After all of the PBMC samples were collected, the frequency of circulating Tfh, defined as CD3$^+$CD4$^+$CXCR5$^+$ lymphocytes, and the expression of CD49a on these cells, were measured using flow cytometry[53]. Briefly, lymphocytes were firstly identified from PBMCs on the basis of their forward (FSC) and sideward (SSC) light scatter properties. Afterward, 7-AAD- CD3$^+$ lymphocytes (alive T cells), CD3$^+$CD4$^+$ T cells, CD3$^+$CD4$^+$CXCR5$^+$ cells (circulating Tfh), and CD3$^+$CD4$^+$CXCR5$^+$CD49a$^+$ (defined as CD49a$^+$ Tfh), were subsequently quantified using the corresponding antibodies according to the manufacturer's instructions (BD Biosciences). The following antibodies were used: anti-CD3, anti-CD4, anti-CXCR5, and anti-CD49a. Of note, Dead cells were excluded using 7-amino-actinomycin D (7-ADD). Samples were acquired on BD LSRFortessa X-20 Flow Cytometer Analyses. Analysis was performed with FlowJo software. The gating strategy is shown in Supplementary Fig. 3.

### External validation

To further investigate the relative abundance of Tfh and its prognostic significance in metastatic NSCLC patients receiving second-line immunotherapy, external datasets were searched in the Gene Expression Omnibus (GEO) (https://www.ncbi.nlm.nih.gov/geo/) under the following criteria: (1) metastatic NSCLC patients receiving second-line PD-1/PD-L1 inhibitors; (2) sample size no less than 50; (3) containing RNA sequencing data; (4) with available survival outcomes. Strategy for searching ("non-small cell lung cancer") [MeSH] AND ("immune checkpoint" or "PD-1" or "PD-L1") [All Fields] AND ("RNA sequencing" or "transcriptome") [All Fields] AND ("Homo sapiens" [Organism]). GSE161537 was identified, which contained targeted RNA sequencing data using formalin-fixed paraffin-embedded biopsies or archival surgically resected specimens collected prior to treatment initiation from 82 metastatic NSCLC patients treated with second-line anti-PD-1/PD-L1 therapy[17,18]. The abundance of infiltrating Tfh in GSE161537 was estimated using CIBERSORT and the association between the frequency of infiltrating Tfh and OS was determined using log-rank test.

### Statistical analyses

The trial was designed to enroll 56 evaluable patients based on the following hypothesis: $H_0$ (null) with an ORR ≤ 20% by Checkmate 017 and Checkmate 057[19,20], $H_1$ (alternative) with an ORR ≥ 38%. If ≥17 patients out of 56 evaluated had an objective response, then $H_0$ will be rejected in favor of $H_1$. This sample size had at least 90% power to reject $H_0$ if the ORR was 38% or more with a one-sided type I error rate of 5%.

The confidence intervals (CIs) of ORR, DCR, and ASR were calculated by the Clopper–Pearson method. Of note, since a one-sided significance level (type I error rate) of 5% was adopted for the sample

size calculation, a two-sided 90% CI of the primary endpoint (ORR in all evaluable patients) was calculated. For other parameters, a two-sided 95% CI was used for the convenience of inter-study comparisons. The survival outcomes were generated using the Kaplan–Meier method and compared using the log-rank test. The safety profile was generally summarized using descriptive statistics. Continuous variables were summarized as medians with interquartile ranges (IQRs), and categorical variables were reported as counts and frequencies (*n*%). For continuous variables adhering to a normal distribution, the significance was evaluated using the paired *t*-test. For continuous variables not fitting a normal distribution, the significance was evaluated using the Wilcoxon rank sum test. The significance with categorical variables was evaluated using Fisher's exact test. All statistical analyses were performed using R software (R version 4.1.2) and SAS 9.4 (SAS Institute Inc, Cary, NC, USA).

### Reporting summary

Further information on research design is available in the Nature Portfolio Reporting Summary linked to this article.

## Data availability

The RNA sequencing data are available in the GSA-Human database with accession code HRA006932; the dataset is under restricted access for ethical and privacy concerns. Access can be granted through the Data Access Committees (DAC) of the GSA-Human database (DAC NO.: HDAC003809), with an estimated response time of about fifteen working days for access requests. Upon approval, the data will be accessible for a duration of 6 months. Applicants may also directly contact the corresponding author. Other de-identified individual data could be obtained by contacting the corresponding author. The study protocol has been previously published[12]. The publicly available data used in this study are available in the GEO database under accession code GSE161537. The remaining data have been provided within the Article and its Supplementary Information. Source data are provided with this paper.

## References


1. Lahiri, A. et al. Lung cancer immunotherapy: progress, pitfalls, and promises. *Mol. Cancer* **22**, 40 (2023).
2. Yang, Y. et al. Efficacy and safety of Sintilimab plus pemetrexed and platinum as first-line treatment for locally advanced or metastatic nonsquamous NSCLC: a randomized, double-blind, phase 3 study (Oncology pRogram by InnovENT anti-PD-1-11). *J. Thorac. Oncol.* **15**, 1636–1646 (2020).
3. Zhou, C. et al. Sintilimab plus platinum and gemcitabine as first-line treatment for advanced or metastatic squamous NSCLC: results from a randomized, double-blind, phase 3 trial (ORIENT-12). *J. Thorac. Oncol.* **16**, 1501–1511 (2021).
4. Passaro, A., Brahmer, J., Antonia, S., Mok, T. & Peters, S. Managing resistance to immune checkpoint inhibitors in lung cancer: treatment and novel strategies. *J. Clin. Oncol.* **40**, 598–610 (2022).
5. Bernstein, M. B., Krishnan, S., Hodge, J. W. & Chang, J. Y. Immunotherapy and stereotactic ablative radiotherapy (ISABR): a curative approach? *Nat. Rev. Clin. Oncol.* **13**, 516–524 (2016).
6. Theelen, W. et al. Pembrolizumab with or without radiotherapy for metastatic non-small-cell lung cancer: a pooled analysis of two randomised trials. *Lancet Respir. Med.* **9**, 467–475 (2021).
7. Zhou, X. et al. Safety and tolerability of low-dose radiation and stereotactic body radiotherapy + sintilimab for treatment-naive stage IV PD-L1+ non-small cell lung cancer patients. *Clin. Cancer Res.* **29**, 4098–4108 (2023).
8. Shi, Y. et al. Granulocyte-macrophage colony-stimulating factor (GM-CSF) and T-cell responses: what we do and don't know. *Cell Res.* **16**, 126–133 (2006).
9. Golden, E. B. et al. Local radiotherapy and granulocyte-macrophage colony-stimulating factor to generate abscopal responses in patients with metastatic solid tumours: a proof-of-principle trial. *Lancet Oncol.* **16**, 795–803 (2015).
10. Shoushtari, A. N. et al. Pilot study of ONCOS-102 and pembrolizumab: remodeling of the tumor microenvironment and clinical outcomes in anti-PD-1-resistant advanced melanoma. *Clin. Cancer Res.* **29**, 100–109 (2023).
11. Tian, H. et al. A novel cancer vaccine with the ability to simultaneously produce anti-PD-1 antibody and GM-CSF in cancer cells and enhance Th1-biased antitumor immunity. *Signal Transduct. Target Ther.* **1**, 16025 (2016).
12. Ni, J. et al. Sintilimab, stereotactic body radiotherapy and granulocyte-macrophage colony stimulating factor as second-line therapy for advanced non-small cell lung cancer: safety run-in results of a multicenter, single-arm, phase II trial. *Radiat. Oncol.* **16**, 177 (2021).
13. Melssen, M. M. et al. Differential expression of CD49a and CD49b determines localization and function of tumor-infiltrating CD8(+) T cells. *Cancer Immunol. Res.* **9**, 583–597 (2021).
14. Cheuk, S. et al. CD49a expression defines tissue-resident CD8(+) T cells poised for cytotoxic function in human skin. *Immunity* **46**, 287–300 (2017).
15. Huang, C. et al. Boosting humoral and cellular immunity with enhanced STING activation by hierarchical mesoporous metal-organic framework adjuvants. *J. Control Release* **370**, 691–706 (2024).
16. Juno, J. A. et al. Humoral and circulating follicular helper T cell responses in recovered patients with COVID-19. *Nat. Med.* **26**, 1428–1434 (2020).
17. Foy, J. P. et al. Immunologically active phenotype by gene expression profiling is associated with clinical benefit from PD-1/PD-L1 inhibitors in real-world head and neck and lung cancer patients. *Eur. J. Cancer* **174**, 287–298 (2022).
18. Foy, J. P. et al. Datasets for gene expression profiles of head and neck squamous cell carcinoma and lung cancer treated or not by PD1/PD-L1 inhibitors. *Data Brief.* **44**, 108556 (2022).
19. Borghaei, H. et al. Nivolumab versus docetaxel in advanced non-squamous non-small-cell lung cancer. *N. Engl. J. Med.* **373**, 1627–1639 (2015).
20. Brahmer, J. et al. Nivolumab versus docetaxel in advanced squamous-cell non-small-cell lung cancer. *N. Engl. J. Med.* **373**, 123–135 (2015).
21. Wu, Y. L. et al. Nivolumab versus docetaxel in a predominantly Chinese patient population with previously treated advanced NSCLC: CheckMate 078 randomized phase III clinical trial. *J. Thorac. Oncol.* **14**, 867–875 (2019).
22. Shi, Y. et al. Sintilimab versus docetaxel as second-line treatment in advanced or metastatic squamous non-small-cell lung cancer: an open-label, randomized controlled phase 3 trial (ORIENT-3). *Cancer Commun.* **42**, 1314–1330 (2022).
23. Theelen, W. et al. Effect of pembrolizumab after stereotactic body radiotherapy vs pembrolizumab alone on tumor response in patients with advanced non-small cell lung cancer: results of the PEMBRO-RT phase 2 randomized clinical trial. *JAMA Oncol.* **5**, 1276–1282 (2019).
24. Broz, M. L. et al. Dissecting the tumor myeloid compartment reveals rare activating antigen-presenting cells critical for T cell immunity. *Cancer Cell* **26**, 638–652 (2014).
25. Lian, G. Y. et al. Disrupting Smad3 potentiates immunostimulatory function of NK cells against lung carcinoma by promoting GM-CSF production. *Cell Mol. Life Sci.* **81**, 262 (2024).
26. Huang, A. C. et al. T-cell invigoration to tumour burden ratio associated with anti-PD-1 response. *Nature* **545**, 60–65 (2017).

27. Seban, R. D. et al. Baseline metabolic tumor burden on FDG PET/CT scans predicts outcome in advanced NSCLC patients treated with immune checkpoint inhibitors. *Eur. J. Nucl. Med Mol. Imaging* **47**, 1147–1157 (2020).
28. Miyawaki, T. et al. Association between clinical tumor burden and efficacy of immune checkpoint inhibitor monotherapy for advanced non-small-cell lung cancer. *Clin. Lung Cancer* **21**, e405–e414 (2020).
29. Vadhan-Raj, S. et al. Effects of recombinant human granulocyte-macrophage colony-stimulating factor in patients with myelodysplastic syndromes. *N. Engl. J. Med.* **317**, 1545–1552 (1987).
30. Anscher, M. S. et al. Association of radiation therapy with risk of adverse events in patients receiving immunotherapy: a pooled analysis of trials in the US Food and Drug Administration Database. *JAMA Oncol.* **8**, 232–240 (2022).
31. Cytlak, U. M. et al. Immunomodulation by radiotherapy in tumour control and normal tissue toxicity. *Nat. Rev. Immunol.* **22**, 124–138 (2022).
32. Rodriguez-Ruiz, M. E., Vanpouille-Box, C., Melero, I., Formenti, S. C. & Demaria, S. Immunological mechanisms responsible for radiation-induced abscopal effect. *Trends Immunol.* **39**, 644–655 (2018).
33. Qiang M. & Zhang R. Identification of potential immune-related ceRNA regulatory network in UVB-irradiated human skin. *Biotechnol. Genet. Eng. Rev.* 1–24 https://doi.org/10.1080/02648725.2023.2175501 (2023).
34. Kim, H., Kang, J. S. & Lee, W. J. The production IL-21 and VEGF in UVB-irradiated human keratinocyte cell line, HaCaT. *Immune Netw.* **10**, 75–80 (2010).
35. Cui, C. et al. Neoantigen-driven B cell and CD4 T follicular helper cell collaboration promotes anti-tumor CD8 T cell responses. *Cell* **184**, 6101–18.e13 (2021).
36. Niogret, J. et al. Follicular helper-T cells restore CD8(+)-dependent antitumor immunity and anti-PD-L1/PD-1 efficacy. *J. Immunother. Cancer* **9**, e002157 (2021).
37. Cho, J. W. et al. Dysregulation of T(FH)-B-T(RM) lymphocyte cooperation is associated with unfavorable anti-PD-1 responses in EGFR-mutant lung cancer. *Nat. Commun.* **12**, 6068 (2021).
38. Liu, W. et al. An immune cell map of human lung adenocarcinoma development reveals an anti-tumoral role of the Tfh-dependent tertiary lymphoid structure. *Cell Rep. Med.* **5**, 101448 (2024).
39. Oja, A. E. et al. Functional heterogeneity of CD4(+) tumor-infiltrating lymphocytes with a resident memory phenotype in NSCLC. *Front. Immunol.* **9**, 2654 (2018).
40. Dadi, S. et al. Cancer immunosurveillance by tissue-resident innate lymphoid cells and innate-like T cells. *Cell* **164**, 365–377 (2016).
41. Reilly, E. C. et al. T(RM) integrins CD103 and CD49a differentially support adherence and motility after resolution of influenza virus infection. *Proc. Natl Acad. Sci. USA* **117**, 12306–12314 (2020).
42. Bromley, S. K. et al. CD49a regulates cutaneous resident memory CD8(+) T cell persistence and response. *Cell Rep.* **32**, 108085 (2020).
43. Wang, Y. et al. Exosomal PD-L1 predicts response with immunotherapy in NSCLC patients. *Clin. Exp. Immunol.* **208**, 316–322 (2022).
44. Chen, G. et al. Exosomal PD-L1 contributes to immunosuppression and is associated with anti-PD-1 response. *Nature* **560**, 382–386 (2018).
45. Yuen, K. C. et al. High systemic and tumor-associated IL-8 correlates with reduced clinical benefit of PD-L1 blockade. *Nat. Med.* **26**, 693–698 (2020).
46. Schoenfeld, J. D. et al. Durvalumab plus tremelimumab alone or in combination with low-dose or hypofractionated radiotherapy in metastatic non-small-cell lung cancer refractory to previous PD(L)-1 therapy: an open-label, multicentre, randomised, phase 2 trial. *Lancet Oncol.* **23**, 279–291 (2022).
47. Chen, Y., Gao, M., Huang, Z., Yu, J. & Meng, X. SBRT combined with PD-1/PD-L1 inhibitors in NSCLC treatment: a focus on the mechanisms, advances, and future challenges. *J. Hematol. Oncol.* **13**, 105 (2020).
48. Dennis, G. Jr. et al. DAVID: database for annotation, visualization, and integrated discovery. *Genome Biol.* **4**, P3 (2003).
49. Newman, A. M. et al. Robust enumeration of cell subsets from tissue expression profiles. *Nat. Methods* **12**, 453–457 (2015).
50. Chen, B., Khodadoust, M. S., Liu, C. L., Newman, A. M. & Alizadeh, A. A. Profiling tumor infiltrating immune cells with CIBERSORT. *Methods Mol. Biol.* **1711**, 243–259 (2018).
51. Luca, B. A. et al. Atlas of clinically distinct cell states and ecosystems across human solid tumors. *Cell* **184**, 5482–96.e28 (2021).
52. Steen, C. B., Luca, B. A., Alizadeh, A. A., Gentles, A. J. & Newman, A. M. Profiling cellular ecosystems at single-cell resolution and at scale with EcoTyper. *Methods Mol. Biol.* **2629**, 43–71 (2023).
53. Lin, X. et al. Follicular helper T cells remodel the immune microenvironment of pancreatic cancer via secreting CXCL13 and IL-21. *Cancers* **13**, 3678 (2021).

## Acknowledgements

This work was supported by the Clinical Research Plan of SHDC [Grant No. SHDC2020CR4010], CSCO foundation [Grant No. Y-XD2019-050], and the Shanghai Municipal Health Commission [Grant No. 20194Y0501]. The funding body had no role in the conceptualization, design, data collection, analysis, decision to publish, or preparation of the manuscript. We thank the patients and their families for participating in this clinical trial. We also thank the Innovent Biologics (Suzhou) Co. Ltd and Xiamen Amoytop Biotech Co., Ltd for providing the corresponding drugs.

## Author contributions

J.J. Ni and Z.F. Zhu contributed conceptualization, data curation, statistical analysis, writing—original draft and writing—review and editing; X. F. Wang contributed to analysis and interpretation, statistical analysis, writing—original draft and writing—review and editing; L. Wu, X.H. Ai, Q. Chu, C.B. Han, X.R. Dong, Y. Zhou, Y.C. Pang contributed to data curation and writing—review and editing.

## Competing interests

The authors declare no competing interests.

## Additional information

**Supplementary information** The online version contains supplementary material available at https://doi.org/10.1038/s41467-024-51807-7.

**Correspondence** and requests for materials should be addressed to Zhengfei Zhu.

**Peer review information** *Nature Communications* thanks Haihua Yang and the other, anonymous, reviewer(s) for their contribution to the peer review of this work. A peer review file is available.